Analysis and computations for a model of quasi-static deformation of a thinning sheet arising in superplastic forming

Article (Unspecified)

Euro. Jnl of Applied Mathematics (2002), *vol.* 13, *pp.* 403–429.
DOI: 10.1017/S095679250100479X Printed in the United Kingdom

Analysis and computations for a model of quasi-static deformation of a thinning sheet arising in superplastic forming

KLAUS DECKELNICK, CHARLES M. ELLIOTT and VANESSA STYLES

Centre for Mathematical Analysis and Its Applications, School of Mathematical Sciences, University of Sussex, Falmer, Brighton BN1 9QH, UK

(*Received 5 May 2000; revised 11 September 2001*)

We consider a mathematical model for the quasi-static deformation of a thinning sheet. The model couples a first-order equation for the thickness of the sheet to a prescribed curvature equation for the displacement of the sheet. We prove a local in time existence and uniqueness theorem for this system when the sheet can be written as a graph. A contact problem is formulated for a sheet constrained to be above a mould. Finally we present some computational results.

1 Introduction

The forming of thin sheets is an important industrial process. Superplastic materials allow very large plastic deformations with low pressures and thus vacuum molding of a superplastic sheet can yield complex shaped pieces without welding and with little subsequent machining. The situation is that of a sheet (known as the blank) placed over a fixed mould (or die) in such a way that there is an enclosed gap between the sheet and mould. The sheet is then subsequently deformed in such a way as to be pressed against the mould and indeed to take up its shape. This is achieved by reducing the pressure in the gap between sheet and mould. Alternatively one could increase the pressure in the external region above the sheet. A schematic depiction of this configuration is shown in Figure 1 for a mould taking the form of a rectangular channel. Because of the large deformations involved considerable thinning of the sheet takes place. We refer to [1, 2, 4] for more details of the industrial applications and for finite element modelling. An important requirement for mathematical modelling of the process is the determination of the final sheet thickness.

In Chapman et al. [3] a simplified mathematical model is proposed for the process of vacuum superplastic forming for thin sheets. Rather than using a power law stress strain relation (cf [1]) the authors assume that the sheet is always in a critically plastic state. Using an asymptotic analysis they derive a rather simple equation which balances the curvature of the centreline of the sheet with the ratio of the applied pressure and varying sheet thickness. This is then coupled to an evolution equation for the thickness derived from local conservation of mass. An interesting feature of the model is its rate independence. The shape and thickness of the sheet are independent of the rate at

which the pressure increases. The model can also be solved backwards in time as we describe later. This may be useful in solving the inverse problem of determining shape and thickness. This is important in the aerospace industry process of net-shape forming in which the final shape of the part is determined by the mould and the desired thickness of the part is to be achieved by pre-contouring of the blank, see [4].

In order to fix ideas, let us consider an infinitely long mould with a uniform cross-section, which is the boundary of an open set $\mathscr{M} \subset \mathbb{R}^2$. Furthermore the cross-section of the sheet is a curve $\Gamma = \Gamma(t)$. We assume that Γ is fixed at two points $x^i_{\mathscr{M}}, i = 1, 2$ on the boundary of the mould $\partial\mathscr{M}$ and to lie above $\partial\mathscr{M}$. For convenience we think of $\partial\mathscr{M}$ as being extended smoothly upwards beyond the points $x^1_{\mathscr{M}}$ and $x^2_{\mathscr{M}}$, see Figure 2. We denote by $\boldsymbol{\nu}_{\mathscr{M}}(\mathbf{x})$ the unit exterior normal to $\partial\mathscr{M}$ for $\mathbf{x} \in \partial\mathscr{M}$ and by $\boldsymbol{\tau}(\mathbf{x}), \boldsymbol{\nu}(\mathbf{x}),\ \mathbf{x} \in \Gamma$ the unit tangent and unit normal to Γ respectively. These are oriented in such a way that $\det(\boldsymbol{\tau}(\mathbf{x}), \boldsymbol{\nu}(\mathbf{x})) = 1$.

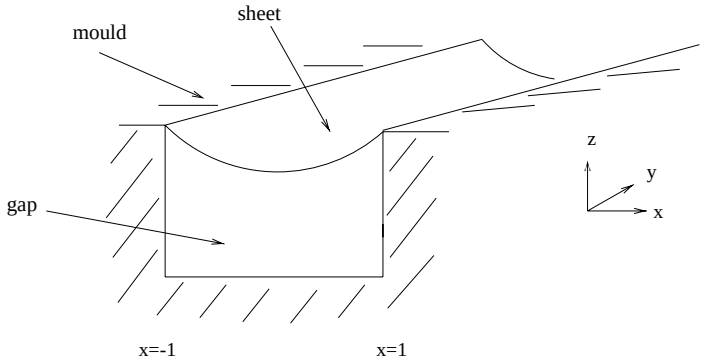

FIGURE 1. Fixed sheet: z=u(x,t)

As long as $\Gamma(t)$ is strictly above $\partial\mathscr{M}$, which we shall call the mould-free case, the authors derive in [3] the following quasi-static equation for elastic/plastic deformation

$$P = d\kappa, \qquad \text{on } \Gamma(t), \tag{1.1}$$

where $P = P(t)$ denotes a time dependent increasing prescribed pressure difference across the sheet, d is the thickness of the sheet and κ is the curvature of Γ. Here we have followed [3] and used dimensionless variables where the lengths have been scaled with respect to a typical value L^* for the width of the mould. Denoting by D^* a typical thickness of the sheet we have that $\epsilon = \frac{D^*}{L^*}$ is a small parameter and the dimensionless thickness is ϵd where d is of order one. The pressure is scaled with $\epsilon\sigma^*$, where σ^* is the material yield stress and is the only material parameter in the model. The model is completed by assuming that

a) mass is conserved locally;
b) material flows normal to the curve. (1.2)

The situation changes if material reaches the mould wall $\partial\mathscr{M}$. In order to describe, how (1.1) has to be modified, we introduce

$$\mathbf{R} := (\kappa - F)\boldsymbol{\nu}(\mathbf{x}), \quad \mathbf{x} \in \Gamma, \tag{1.3}$$

with $F = P/d > 0$. $\mathbf{R}$ is the difference of the normal force $F\boldsymbol{v}(\mathbf{x})$ on the sheet due to the pressure difference and the resistive force $\kappa\boldsymbol{v}(\mathbf{x})$. Away from the boundaries of the mould where the sheet is unconstrained we have for $\mathbf{x} \in \Gamma(t)$

$$\mathbf{x} \in \mathscr{M}, \quad \mathbf{R} = 0 \tag{1.4}$$

whereas on the boundary of the mould

$$\mathbf{x} \in \partial\mathscr{M}, \quad \mathbf{R} \cdot \boldsymbol{v}_{\mathscr{M}}(\mathbf{x}) \geqslant 0. \tag{1.5}$$

The second condition in (1.5) is a condition on the direction of the reaction force on the sheet due to the mould where there is contact. Together (1.4) and (1.5) can be viewed as a complementarity system. Finally, we make the hypothesis, suggested in [3], that once the sheet hits the mould wall it remains attached to the mould and cannot move thereafter.

In order to study the evolution of $\Gamma(t)$ analytically or numerically a suitable description of the curve is needed. In [3] they set the position of the sheet to be given parametrically by

$$\mathbf{x}(p,t) = (x(p,t), z(p,t)), \quad p \in [0,1], \tag{1.6}$$

where p parameterises the curve and t is time. In view of our choice of orientation we have $\boldsymbol{v}(\mathbf{x}) = \frac{\mathbf{x}_p^{\perp}}{|\mathbf{x}_p|}$, where $\mathbf{a}^{\perp} = (-a_2, a_1)$ for $\mathbf{a} = (a_1, a_2) \in \mathbb{R}^2$. Then (1.1) becomes

$$P(t) = d\,\frac{\mathbf{x}_{pp}}{|\mathbf{x}_p|^2} \cdot \frac{\mathbf{x}_p^{\perp}}{|\mathbf{x}_p|}, \quad p \in [0,1], t \in [0,T], \tag{1.7}$$

while the conditions in (1.2) translate into

$$\frac{\partial}{\partial t}\Big(d(p,t)|\mathbf{x}_p|\Big) = 0, \qquad p \in [0,1], t \in [0,T] \tag{1.8}$$

$$\mathbf{x}_t(p,t) \cdot \mathbf{x}_p(p,t) = 0, \qquad p \in [0,1], t \in [0,T]. \tag{1.9}$$

Furthermore, appropriate boundary and initial conditions have to be added.

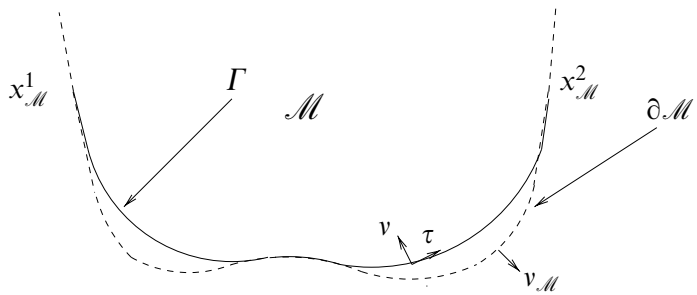

FIGURE 2. The cross-section $\mathscr{M}$

Having derived (1.1) and (1.2) Chapman et al. in [3] (i) give the exact solution when d is a given constant for all time i.e. arcs of circles, (ii) give the exact solution for thinning with d being space-independent, again circular arcs, (iii) derive a nontrivial similarity solution and (iv) derive a numerical discretization and perform calculations.

In this paper we give a reformulation of the problem. The position of the sheet is determined by the two components $(x(p,t), z(p,t))$. However, numerical experiments suggest that (at least locally in time) $\Gamma(t)$ can be written as a graph $u(\cdot,t)$. In § 2 we shall derive the system satisfied by u and the thickness d that corresponds to the problem (1.1), (1.2). We obtain a first order equation for d which is coupled to a prescribed curvature equation for u. This approach has several advantages: it can easily be generalized to fully three-dimensional sheets (see § 2.2) and there is a natural formulation of the contact problem (1.4), (1.5) as an obstacle problem (see § 2.3). Furthermore, we are able to prove a short time existence and uniqueness result for the one-dimensional mould-free problem. The proof and further properties of the solution will be presented in § 3. In § 4 we present numerical discretizations for the graph formulations derived in § 2 both for the mould-free and the contact problem. For the contact problem we encounter the difficulty that the solution loses the property of being a graph at a certain time. Our way around this problem is a suitable rotation of coordinates which allows us to follow the evolution in the graph setting. An alternative method, which avoids the change of coordinates, relies on the parametric approach. To this end, in § 5 we return to (1.4), (1.5) and rewrite it as a complementarity system. We solve this system numerically with the help of a fixed point iteration and compare the results with those obtained from the graph approach. We display some computational results in § 6 and finally we present some conclusions in § 7.

2 A graph formulation of the model

2.1 The one-dimensional mould-free model

For the one-dimensional mould-free problem we set $\mathcal{M} = \{(x,z) \in \mathbb{R}^2 \mid -1 < x < 1\}$ and $x^1_{\mathcal{M}} = (-1,0)$, $x^2_{\mathcal{M}} = (1,0)$. We assume that the sheet can be written as a graph $\Gamma(t) = \{(x, u(x,t)) \mid x \in \Omega = (-1,1)\}$ with $u(-1,t) = u(1,t) = 0$ (see Figure 1).

We set the thickness of the sheet to be $d(x,t)$, $x \in \Omega$ and noting that $\kappa = \dfrac{\partial}{\partial x}\Big(\dfrac{u_x}{\sqrt{1+u_x^2}}\Big)$ we obtain from (1.1)

$$\frac{\partial}{\partial x}\left(\frac{u_x(.,t)}{\sqrt{1+u_x(.,t)^2}}\right) = \frac{P(t)}{d(.,t)} \quad \text{in } \Omega. \tag{2.1}$$

We now write

$$\Gamma(t) \ni (x,z) = \Psi(A,t) = (a(A,t), u(a(A,t),t)), \tag{2.2}$$

where A defines a point on the sheet at the time $t = 0$ and $a = a(A,t)$ defines the x coordinate of this point at time t such that

$$a(A,0) = A.$$

The unit tangent vector to the graph of u is $\boldsymbol{\tau} = \frac{(1,u_x)}{\sqrt{1+u_x^2}}$. Recalling (1.2) b) we have

$$0 = \Psi_t \cdot \boldsymbol{\tau} = (a_t, u_t + u_x a_t) \cdot \frac{(1,u_x)}{\sqrt{1+u_x^2}} = \frac{a_t + u_x^2 a_t + u_x u_t}{\sqrt{1+u_x^2}},$$

which implies that

$$v := a_t = \frac{-u_x u_t}{1+u_x^2}. \tag{2.3}$$

Finally since mass is conserved and the density is constant it follows that we have conservation of area and thus for any points $A_1 \in \Omega,\ A_2 \in \Omega$ we have

$$\frac{d}{dt}\int_{a(A_1,t)}^{a(A_2,t)} d(x,t)\sqrt{1+u_x^2}\,dx = 0.$$

Setting $D(A,t) = d(a(A,t),t)$ as well as $\mathscr{S}(A,t) = \sqrt{1+u_x^2(a(A,t),t)}$ it follows that

$$\frac{d}{dt}\int_{A_1}^{A_2} (D\,\mathscr{S} a_A)(A,t)\,dA = 0$$

and therefore, since A_1 and A_2 were arbitrary

$$D_t \mathscr{S} a_A + D\mathscr{S}_t a_A + D\mathscr{S} a_{At} = 0. \tag{2.4}$$

Next, differentiating (2.3) with respect to A we obtain

$$\frac{a_{At}}{a_A} = \frac{-(1+u_x^2)(u_{xx}u_t + u_{xt}u_x) + 2u_x^2 u_t u_{xx}}{(1+u_x^2)^2}.$$

Combining this with (2.4) and the identity $\mathscr{S}_t = (1+u_x^2)^{-1/2}u_x(u_{xt}+u_{xx}a_t)$ it follows that

$$\begin{aligned} d_t + d_x a_t = D_t &= -D\frac{\mathscr{S}_t}{\mathscr{S}} - D\frac{a_{At}}{a_A} \\ &= -d\,\frac{u_x(u_{xt}+u_{xx}a_t)}{1+u_x^2} + d\frac{(1+u_x^2)(u_{xx}u_t+u_{xt}u_x) - 2u_x^2 u_t u_{xx}}{(1+u_x^2)^2} \\ &= \frac{d u_t u_{xx}}{(1+u_x^2)^2}. \end{aligned}$$

Inserting (1.1) and (2.3) into the above relation we arrive at

$$d_t - \frac{u_x u_t}{1+u_x^2} d_x = \frac{d u_t \kappa}{\sqrt{1+u_x^2}} = \frac{u_t P(t)}{\sqrt{1+u_x^2}}. \tag{2.5}$$

Thus our one-dimensional evolutionary model in the absence of a mould takes the form of (2.1), (2.3) and (2.5) together with initial and boundary data

$$d(x,0) = d_0(x) \qquad x \in (-1,1), \tag{2.6}$$

$$u(-1,t) = u(1,t) = 0 \qquad t \in (0,T). \tag{2.7}$$

If we assume that d_0 is symmetric with respect to $x = 0$ this model can be written in the following form

$$\frac{u_{xx}}{(1+u_x^2)^{3/2}} = \frac{P(t)}{d} \qquad x \in (0,1), t \in (0,T) \tag{2.8}$$

$$u_x(0,t) = 0, u(1,t) = 0 \qquad t \in (0,T) \tag{2.9}$$

$$d_t - \frac{u_x u_t d_x}{1+u_x^2} = \frac{P(t)u_t}{\sqrt{1+u_x^2}} \qquad x \in (0,1), t \in (0,T) \tag{2.10}$$

$$d(x,0) = d_0(x) \qquad x \in (0,1). \tag{2.11}$$

Henceforth we shall use (2.8)–(2.11) when studying the one-dimensional mould-free problem.

We also observe the following property of the above systems: suppose that $P(0) = 0$ and that $P'(t) > 0$ for $t > 0$ and let $\tilde{t} = P(t)$ as well as $(\tilde{u}, \tilde{d})(x, \tilde{t}) = (u, d)(x, t)$. Then

$$u_t = \tilde{u}_{\tilde{t}} P'(t), \quad d_t = \tilde{d}_{\tilde{t}} P'(t)$$

and $(\tilde{u}, \tilde{d})$ satisfy (2.8)–(2.11) with $P(t)$ replaced by $\tilde{t}$. Hence the solution is rate independent in the sense that it depends only on the order of the values of $P(t) \in [0, P(T))$ and not the rate at which $P(\cdot)$ changes. A similar remark applies to the parametric approach.

2.2 The two-dimensional model

For the two-dimensional mould-free problem we set $\Omega = (0,1) \times (0,1)$ and we take the sheet to be the graph $(\mathbf{x}, u(\mathbf{x}, t))$ for all $\mathbf{x} = (x, y) \in \Omega$, with $u(\mathbf{x}, t) = 0$ for all $\mathbf{x} \in \partial\Omega$ and we set its thickness to be $d(\mathbf{x}, t)$ for all $\mathbf{x} \in \Omega$. Note that the sheet $\Gamma(t)$ is now a two-dimensional surface and the equation (1.1) is replaced by $P = dH$ on $\Gamma(t)$ (cf. [3], p. 240), where H is the mean curvature of $\Gamma(t)$. Thus we have

$$\nabla \cdot \left(\frac{\nabla u(.,t)}{\sqrt{1 + |\nabla u(.,t)|^2}} \right) = \frac{P(t)}{d} \qquad \mathbf{x} \in \Omega, t \in (0, T). \tag{2.12}$$

We now write $\Gamma(t) \ni \Psi(\mathbf{A}, t) = (\mathbf{a}(\mathbf{A}, t), u(\mathbf{a}(\mathbf{A}, t), t)) = (a_1(\mathbf{A}, t), a_2(\mathbf{A}, t), U(\mathbf{A}, t))$, where $\mathbf{A} = (A_1, A_2)$, $\mathbf{a}(\mathbf{A}, 0) = \mathbf{A}$ and $U(\mathbf{A}, t) = u(\mathbf{a}(\mathbf{A}, t), t)$. Noting that the sheet evolves in the normal direction we have

$$\Psi_t \cdot (1, 0, u_x) = 0, \quad \Psi_t \cdot (0, 1, u_y) = 0.$$

Since $\Psi_t = (a_{1t}, a_{2t}, u_x a_{1t} + u_y a_{2t} + u_t)$ this can be rewritten as

$$\begin{pmatrix} 1 + u_x^2 & u_x u_y \\ u_x u_y & 1 + u_y^2 \end{pmatrix} \begin{pmatrix} a_{1t} \\ a_{2t} \end{pmatrix} = \begin{pmatrix} -u_x u_t \\ -u_y u_t \end{pmatrix}.$$

Thus,

$$\begin{aligned} \mathbf{v} = \begin{pmatrix} a_{1t} \\ a_{2t} \end{pmatrix} &= \frac{1}{(1 + u_x^2)(1 + u_y^2) - u_x^2 u_y^2} \begin{pmatrix} 1 + u_y^2 & -u_y u_x \\ -u_x u_y & 1 + u_x^2 \end{pmatrix} \begin{pmatrix} -u_x u_t \\ -u_y u_t \end{pmatrix} \\ &= \frac{-u_t}{1 + |\nabla u|^2} \nabla u. \end{aligned} \tag{2.13}$$

Finally since mass is conserved and the density is constant it follows that we have conservation of volume and thus for any region $M(t)$ at time t, where $M(0)$ is the region in Ω that a specified portion of the sheet occupies at $t = 0$, we have

$$\frac{d}{dt} \int_{M(t)} d \sqrt{1 + |\nabla u|^2} d\mathbf{x} = 0. \tag{2.14}$$

So that the region of integration is independent of time we transform (2.14) into the initial coordinates $\mathbf{A}$ to obtain

$$\frac{d}{dt} \int_{M(0)} D \, \mathscr{S} \det J \, d\mathbf{A} = 0,$$

where $D(\mathbf{A},t) = d(\mathbf{a}(\mathbf{A},t),t)$, $(J_{ij}) = (\frac{\partial \mathbf{a}_i}{\partial \mathbf{A}_j})$ and $\mathscr{S}(\mathbf{A},t) = \sqrt{1+|\nabla u|^2} = \sqrt{1+|J^{-T}\nabla_{\mathbf{A}}U|^2}$. Noting that $\frac{\partial}{\partial t}(\det J) = \nabla\cdot\mathbf{v}\det J$ this implies

$$D_t\mathscr{S} + D\mathscr{S}_t + D\mathscr{S}\nabla\cdot\mathbf{v} = 0.$$

Observing that

$$\mathscr{S}_t = \mathbf{v}\cdot\nabla\big(\sqrt{1+|\nabla u|^2}\big) + \frac{\nabla u\cdot\nabla u_t}{\sqrt{1+|\nabla u|^2}}$$

and arguing in a similar way as for the one-dimensional case we may continue

$$\begin{aligned} d_t + \mathbf{v}\cdot\nabla d = D_t &= -D\frac{\mathscr{S}_t}{\mathscr{S}} - D\,\nabla\cdot\mathbf{v} \\ &= -\frac{d}{\sqrt{1+|\nabla u|^2}}\,\mathbf{v}\cdot\nabla\big(\sqrt{1+|\nabla u|^2}\big) - \frac{d\,\nabla u\cdot\nabla u_t}{1+|\nabla u|^2} + d\,\nabla\cdot\big(\frac{u_t\nabla u}{1+|\nabla u|^2}\big) \\ &= \frac{d\,u_t}{\sqrt{1+|\nabla u|^2}}\nabla\cdot\left(\frac{\nabla u}{\sqrt{1+|\nabla u|^2}}\right) = \frac{u_t P(t)}{\sqrt{1+|\nabla u|^2}}. \end{aligned}$$

In conclusion, the two-dimensional model is described by the system

$$\nabla\cdot\left(\frac{\nabla u}{\sqrt{1+|\nabla u|^2}}\right) = \frac{P(t)}{d} \qquad \mathbf{x}\in\Omega, t\in(0,T) \tag{2.15}$$

$$u(x,0) = 0 \qquad \mathbf{x}\in\Omega \tag{2.16}$$

$$d_t - \frac{u_t\nabla u\cdot\nabla d}{1+|\nabla u|^2} = \frac{P(t)u_t}{\sqrt{1+|\nabla u|^2}} \qquad \mathbf{x}\in\Omega, t\in(0,T) \tag{2.17}$$

$$d(x,0) = d_0(x) \qquad \mathbf{x}\in\Omega. \tag{2.18}$$

2.3 A graph formulation of the contact problem

In the setting of Section 2.2 where the sheet is a graph $z = u(x,y,t)$ not in contact with the vertical mould walls but constrained to lie above a lower mould wall $z = \psi(x,y)$, the conditions (1.4), (1.5) become

$$u \geqslant \psi, \quad -\nabla\cdot\left(\frac{\nabla u}{\sqrt{1+|\nabla u|^2}}\right) + \frac{P(t)}{d} \geqslant 0$$

$$\left(\frac{P(t)}{d} - \nabla\cdot\left(\frac{\nabla u}{\sqrt{1+|\nabla u|^2}}\right)\right)(u-\psi) = 0.$$

This can be posed as the following variational inequality of obstacle type

$$\int_\Omega \frac{\nabla u\cdot(\nabla\eta - \nabla u)}{\sqrt{1+|\nabla u|^2}}d\mathbf{x} + \int_\Omega \frac{P(t)}{d}(\eta - u)d\mathbf{x} \geqslant 0 \quad \forall\ \eta\in K, \tag{2.19}$$

where

$$K = \{\eta\in H^1(\Omega) : \eta(\mathbf{x}) \geqslant \psi(\mathbf{x}), \quad \forall\ \mathbf{x}\in\Omega, \quad \eta(\mathbf{x}) = 0 \ \ \forall\ \mathbf{x}\in\partial\Omega\}.$$

Finally the equation for d remains (2.17). This means that the sheet is motionless and does not thin when in contact with the mould. The problem in one-space dimension is analogous.

3 Existence theory

In this section we prove a local existence result for (2.8)–(2.11). In view of the observation made at the end of Section 2.1 we shall assume without loss of generality that $P(t) = t$. Furthermore recall that

$$C^{1,1}[0,1] = \{d \in C^1[0,1] \mid d' \text{ is Lipschitz continuous}\}.$$

Theorem 1 *Suppose $d_0 \in C^{1,1}[0,1]$ with $d_0(x) \geqslant c_0 > 0$ for all $x \in [0,1]$. There exists $T = T(d_0, c_0) > 0$ such that (2.8)–(2.11) has a unique solution (d,u) satisfying*

$$d, u \in C^1([0,1] \times [0,T]), \quad u(.,t) \in C^2([0,1]) \text{ for all } t \in [0,T]. \tag{3.1}$$

Proof The proof uses a fixed point argument for a contraction mapping. Consider the metric space

$$\mathscr{B} := \{\eta \in C^1([0,1] \times [0,T]) : ||\eta||_{\mathscr{B}} \leqslant R,\ \eta(x,t) \geqslant \frac{c_0}{2}, \quad \forall\ (x,t) \in [0,1] \times [0,T]\} \tag{3.2}$$

with $||\eta||_{\mathscr{B}} = ||\eta||_{C^1([0,1]\times[0,T])}$, where R will be determined later and

$$T \leqslant \frac{c_0}{2\sqrt{2}}. \tag{3.3}$$

There will be additional restrictions on T in the course of the proof.

We define a mapping $\mathscr{F} : \mathscr{B} \to C^1([0,1] \times [0,T])$ in the following way: given $d \in \mathscr{B}$, for every $t \in [0,T]$, let $u(\cdot,t)$ be the unique solution of

$$\frac{\partial}{\partial x}\left(\frac{u_x(.,t)}{\sqrt{1+u_x^2(.,t)}}\right) = \frac{t}{d} \quad \text{in } [0,1], \tag{3.4}$$

$$u_x(0,t) = u(1,t) = 0. \tag{3.5}$$

The solution is given by the formula

$$u(x,t) = -\int_x^1 \frac{t\alpha(z,t)}{\sqrt{1-t^2\alpha^2(z,t)}}dz, \tag{3.6}$$

where

$$\alpha(x,t) = \int_0^x \frac{1}{d(z,t)}dz.$$

Note that $u(.,t)$ is well-defined because

$$1 - t^2\alpha^2(x,t) \geqslant 1 - \frac{4T^2}{c_0^2} \geqslant \frac{1}{2} \tag{3.7}$$

by (3.3). Recalling the definition of $\mathscr{B}$ we can calculate the following expressions for the derivatives of u:

$$\left.\begin{aligned} u_x(x,t) &= \frac{t\alpha(x,t)}{\sqrt{1-t^2\alpha^2(x,t)}} \\ u_{xx}(x,t) &= \frac{t}{d(x,t)}(1+u_x^2(x,t))^{3/2} \\ u_t(x,t) &= -\int_x^1 \frac{\alpha(z,t)}{(1-t^2\alpha^2(z,t))^{3/2}}dz + t\int_x^1 \frac{\beta(z,t)}{(1-t^2\alpha^2(z,t))^{3/2}}dz \\ u_{xt}(x,t) &= \frac{\alpha(x,t)-t\beta(x,t)}{(1-t^2\alpha^2(x,t))^{3/2}}, \end{aligned}\right\} \tag{3.8}$$

where

$$\beta(x,t) = \int_0^x \frac{d_t(z,t)}{d^2(z,t)}dz.$$

Clearly,

$$\sup_{t\in[0,T]} \|u_x(.,t)\|_{C^1[0,1]} \leqslant TM \tag{3.9}$$

$$\sup_{t\in[0,T]} \|u_t(.,t)\|_{C^2[0,1]} + \sup_{t\in[0,T]} \|u_{xxx}(.,t)\|_{C^0[0,1]} \leqslant M(1+TR). \tag{3.10}$$

Here and in what follows, M will denote a constant, which only depends on c_0 and which may change from line to line.

Next, we define $e(x,t)$ to be the solution of the initial value problem

$$e_t + b(x,t)e_x = g(x,t), \quad x\in[0,1],\ 0\leqslant t\leqslant T, \tag{3.11}$$

$$e(x,0) = d_0(x), \quad x\in[0,1], \tag{3.12}$$

where

$$b(x,t) := -\frac{u_x(x,t)u_t(x,t)}{1+u_x^2(x,t)}, \quad g(x,t) := \frac{tu_t(x,t)}{\sqrt{1+u_x^2(x,t)}}. \tag{3.13}$$

The existence of a unique solution $e\in C^1([0,1]\times[0,T])$ of (3.11)–(3.12) follows from the method of characteristics, which also yields the following formula for the solution:

$$e(x,t) = d_0(\lambda(0;x,t)) + \int_0^t g(\lambda(s;x,t),s)ds, \tag{3.14}$$

where the characteristics $\lambda(s) = \lambda(s;x,t)$ are defined by

$$\dot\lambda(s) = b(\lambda(s),s), \quad s\in[0,T], \quad \lambda(t) = x. \tag{3.15}$$

We note that since $b(0,t) = b(1,t) = 0$ for all $t\in[0,T]$, it follows that $\lambda(s)\in[0,1]$ for all $x\in[0,1]$ and $t\in[0,T]$.

We now define $\mathscr{F}(d) := e$. Clearly (u,d) is a solution of (2.8)–(2.11) if and only if d is a fixed point of $\mathscr{F}$ and u is given by (3.4), (3.5).

Claim $\mathscr{F}(\mathscr{B})\subset\mathscr{B}$ and $\mathscr{F}$ is a contraction, provided that T is sufficiently small.

Using (3.10) we have

$$\sup_{t\in[0,T]} \|b(.,t)\|_{C^2[0,1]} \leqslant M(1+TR), \quad \sup_{t\in[0,T]} \|g(.,t)\|_{C^2[0,1]} \leqslant TM(1+TR) \tag{3.16}$$

so that (3.14) implies

$$\frac{c_0}{2} \leqslant e(x,t) \leqslant 2 \sup_{x\in[0,1]} d_0(x) \tag{3.17}$$

provided that

$$TM(1+TR) \leqslant \min\Big(\frac{c_0}{2}, \sup_{x\in[0,1]} d_0(x)\Big). \tag{3.18}$$

Furthermore

$$e_x(x,t) = d_0'(\lambda(0;x,t))\frac{\partial\lambda}{\partial x}(0;x,t) + \int_0^t g_x(\lambda(s;x,t),s)\frac{\partial\lambda}{\partial x}(s;x,t)ds \tag{3.19}$$

where from (3.15) we have $\dfrac{\partial\lambda}{\partial x}(s;x,t)$ satisfies

$$\dot{\frac{\partial\lambda}{\partial x}} = b_x(\lambda(s),s)\,\frac{\partial\lambda}{\partial x}(s),\ s\in[0,T], \qquad \frac{\partial\lambda}{\partial x}(t) = 1. \tag{3.20}$$

From (3.13) and (3.9), (3.10) we infer

$$\Big|\frac{\partial\lambda}{\partial x}(s)\Big| \leqslant 1 + T \sup_{[0,1]\times[0,T]} |b_x| \sup_{\tau\in[0,T]} \Big|\frac{\partial\lambda}{\partial x}(\tau)\Big| \leqslant 1 + TM(1+TR) \sup_{\tau\in[0,T]} \Big|\frac{\partial\lambda}{\partial x}(\tau)\Big|$$

so that

$$\sup_{s\in[0,T]} \Big|\frac{\partial\lambda}{\partial x}(s)\Big| \leqslant 2 \tag{3.21}$$

provided that

$$T \sup_{[0,1]\times[0,T]} |b_x| \leqslant TM(1+TR) \leqslant \frac{1}{2}. \tag{3.22}$$

Thus, (3.19), (3.21) and (3.10) imply

$$|e_x(x,t)| \leqslant 2 \sup_{x\in[0,1]} |d_0'(x)| + 2T \sup_{[0,1]\times[0,T]} |g_x| \leqslant 2 \sup_{x\in[0,1]} |d_0'(x)| + TM(1+TR) \tag{3.23}$$

and finally using (3.11), (3.13), (3.10) and (3.23)

$$\begin{aligned} |e_t(x,t)| &\leqslant |g(x,t)| + |b(x,t)|\,|e_x(x,t)| \\ &\leqslant TM(1+TR) + M(1+TR)\big(2 \sup_{x\in[0,1]} |d_0'(x)| + TM(1+TR)\big) \\ &\leqslant M \sup_{x\in[0,1]} |d_0'(x)| + TM(1+TR)\big(1 + \sup_{x\in[0,1]} |d_0'(x)|\big), \end{aligned}$$

which implies in combination with (3.17) and (3.23)

$$\|e\|_{\mathscr{B}} \leqslant 2 \sup_{x\in[0,1]} d_0(x) + (M+2) \sup_{x\in[0,1]} |d_0'(x)| + TM(1+TR)\big(1 + \sup_{x\in[0,1]} |d_0'(x)|\big).$$

Let us first choose $R > 0$ so large that $2\sup_{x\in[0,1]} d_0(x) + (M+2)\sup_{x\in[0,1]} |d_0'(x)| \leqslant \frac{1}{2}R$. Afterwards choose T so small that $TR \leqslant 1$, (3.18), (3.22) as well as

$$TM(1+TR)\big(1+\sup_{x\in[0,1]}|d_0'(x)|\big) \leqslant \frac{1}{2}R$$

are satisfied. This implies that $e \in \mathscr{B}$, so that $\mathscr{F}(\mathscr{B}) \subset \mathscr{B}$.

We now prove that $\mathscr{F}$ is a contraction mapping. To this end let $d, \hat{d} \in \mathscr{B}$ with $e = \mathscr{F}(d), \hat{e} = \mathscr{F}(\hat{d})$ and we denote by $u,\ \hat{u}$ the solutions of the corresponding elliptic problems. Furthermore, let b, g and $\hat{b}, \hat{g}$ respectively be the functions appearing in (3.13) and $\lambda, \hat{\lambda}$ the corresponding characteristics.

A short calculation shows

$$\sup_{t\in[0,T]} \|(b-\hat{b})(.,t)\|_{C^1[0,1]} + \sup_{t\in[0,T]} \|(g-\hat{g})(.,t)\|_{C^1[0,1]} \leqslant C\|d-\hat{d}\|_{\mathscr{B}}. \tag{3.24}$$

Next, let us derive estimates for the difference between λ and $\hat{\lambda}$. Clearly,

$$(\dot{\lambda}-\dot{\hat{\lambda}})(s) = \big(b(\lambda(s),s) - b(\hat{\lambda}(s),s)\big) + \big(b(\hat{\lambda}(s),s) - \hat{b}(\hat{\lambda}(s),s)\big), \quad s \in [0,T]$$
$$(\lambda-\hat{\lambda})(t) = 0.$$

Thus,

$$|(\lambda-\hat{\lambda})(s)| \leqslant T \sup_{[0,1]\times[0,T]} |b_x| \sup_{\tau\in[0,T]} |\lambda(\tau)-\hat{\lambda}(\tau)| + T \sup_{\tau\in[0,T]} \|(b-\hat{b})(.,\tau)\|_{C^0[0,1]}$$

which implies using (3.22) and (3.24)

$$\sup_{0\leqslant s\leqslant T} |(\lambda-\hat{\lambda})(s)| \leqslant TC\|d-\hat{d}\|_{\mathscr{B}}. \tag{3.25}$$

Recalling (3.20) we have

$$\overbrace{\Big(\frac{\partial\lambda}{\partial x} - \frac{\partial\hat{\lambda}}{\partial x}\Big)}^{\cdot}(s) = b_x(\lambda(s),s)\left(\frac{\partial\lambda}{\partial x}(s) - \frac{\partial\hat{\lambda}}{\partial x}(s)\right) + \big(b_x(\lambda(s),s) - b_x(\hat{\lambda}(s),s)\big)\frac{\partial\hat{\lambda}}{\partial x}(s)$$
$$+\big(b_x(\hat{\lambda}(s),s) - \hat{b}_x(\hat{\lambda}(s),s)\big)\frac{\partial\hat{\lambda}}{\partial x}(s)$$

and

$$\left(\frac{\partial\lambda}{\partial x} - \frac{\partial\hat{\lambda}}{\partial x}\right)(t) = 0.$$

Arguing in a similar way as above we deduce

$$\begin{aligned}
&\sup_{0\leqslant s\leqslant T}\left|\frac{\partial\lambda}{\partial x}(s) - \frac{\partial\hat{\lambda}}{\partial x}(s)\right| \\
&\quad\leqslant TC \sup_{[0,1]\times[0,T]} |b_{xx}| \sup_{s\in[0,T]} |\lambda(s)-\hat{\lambda}(s)| + T \sup_{s\in[0,T]} \|(b-\hat{b})(.,t)\|_{C^1[0,1]} \\
&\quad\leqslant TC\|d-\hat{d}\|_{\mathscr{B}}.
\end{aligned} \tag{3.26}$$

In view of (3.19) we may write

$$\begin{aligned} e_x(x,t) - \hat{e}_x(x,t) &= \Big(d_0'(\lambda(0;x,t)) - d_0'(\hat{\lambda}(0;x,t))\Big)\frac{\partial\lambda}{\partial x}(0;x,t) \\ &\quad + d_0'(\hat{\lambda}(0;x,t))\left(\frac{\partial\lambda}{\partial x}(0;x,t) - \frac{\partial\hat{\lambda}}{\partial x}(0;x,t)\right) \\ &\quad + \int_0^t \Big(g_x(\lambda(s;x,t),s) - \hat{g}_x(\lambda(s;x,t),s)\Big)\frac{\partial\lambda}{\partial x}(s;x,t)ds \\ &\quad + \int_0^t \Big(\hat{g}_x(\lambda(s;x,t),s) - \hat{g}_x(\hat{\lambda}(s;x,t),s)\Big)\frac{\partial\lambda}{\partial x}(s;x,t)ds \\ &\quad + \int_0^t \hat{g}_x(\hat{\lambda}(s;x,t),s)\left(\frac{\partial\lambda}{\partial x}(s;x,t) - \frac{\partial\hat{\lambda}}{\partial x}(s;x,t)\right)ds. \end{aligned}$$

Noting (3.21), (3.24), (3.10), (3.25) and (3.26)

$$\begin{aligned} &|e_x(x,t) - \hat{e}_x(x,t)| \\ &\leqslant \|d_0\|_{C^{1,1}[0,1]}\left(2|\lambda(0;x,t) - \hat{\lambda}(0;x,t)| + \left|\frac{\partial\lambda}{\partial x}(0;x,t) - \frac{\partial\hat{\lambda}}{\partial x}(0;x,t)\right|\right) \qquad (3.27) \\ &\quad + 2T \sup_{s\in[0,T]} \|(g-\hat{g})(.,s)\|_{C^1[0,1]} + 2T \sup_{[0,1]\times[0,T]} |\hat{g}_{xx}| \sup_{s\in[0,T]} |\lambda(s) - \hat{\lambda}(s)| \\ &\quad + T \sup_{[0,1]\times[0,T]} |\hat{g}_x| \sup_{s\in[0,T]} \left|\frac{\partial\lambda}{\partial x}(s) - \frac{\partial\hat{\lambda}}{\partial x}(s)\right| \\ &\leqslant CT\|d - \hat{d}\|_{\mathscr{B}} \end{aligned}$$

for all $x \in [0,1], t \in [0,T]$. Furthermore from (3.11), (3.24) and (3.27) it follows that

$$\begin{aligned} &|e_t(x,t) - \hat{e}_t(x,t)| \qquad (3.28) \\ &\leqslant |b(x,t) - \hat{b}(x,t)||e_x(x,t)| + |\hat{b}(x,t)||e_x(x,t) - \hat{e}_x(x,t)| + |g(x,t) - \hat{g}(x,t)| \\ &\leqslant CT||d - \hat{d}||_{\mathscr{B}} \end{aligned}$$

for all $x \in [0,1], t \in [0,T]$. Finally, observing that

$$e(x,t) - \hat{e}(x,t) = \int_0^t (e_t(x,s) - \hat{e}_t(x,s))ds \qquad (3.29)$$

we deduce from (3.27)–(3.29)

$$||\mathscr{F}(d) - \mathscr{F}(\hat{d})||_{\mathscr{B}} = ||e - \hat{e}||_{\mathscr{B}} \leqslant \frac{1}{2}||d - \hat{d}||_{\mathscr{B}},$$

provided that T is sufficiently small. Thus $\mathscr{F}$ is a contraction mapping and has a fixed point in $\mathscr{B}$ such that $d = \mathscr{F}(d)$. □

Remark 1 Examination of the proof of the theorem reveals that it can be applied to give a local existence uniqueness result backwards in time. This may be useful when studying the inverse problem.

Remark 2 We can derive conditions on the solution so that it can be continued in time. Suppose that the solution (u, d) exists on $[0, t_0)$ and that

$$\inf_{x\in[0,1]} d(x,t) \geqslant c_1 > 0, \quad t_0 \int_0^1 \frac{1}{d(z,t)} dz \leqslant q < 1 \qquad \text{for all } t < t_0. \tag{3.30}$$

Then there exists $\delta = \delta(c_1, q) > 0$ such that the solution can be continued to $[0, t_0 + \delta)$.

Proof We only sketch the argument leaving the details to the reader. By (3.30) and the formula (3.6) for u we can derive bounds analogous to (3.9), (3.10) and (3.16) with constants depending on c_1, q and t_0. Combining these estimates with the representation

$$d(x,t) = d_0(\lambda(0;x,t)) + \int_0^t g(\lambda(s;x,t),s)ds$$

(g as in (3.13)) we are then able to prove that $\|d(.,t)\|_{C^{1,1}[0,1]} \leqslant C$ uniformly in $t < t_0$. In view of Arzela's theorem there exists a sequence $(t_j)_{j\in\mathbb{N}}$, $t_j \nearrow t_0$ and $\bar{d} \in C^{1,1}[0,1]$ such that $d(.,t_j) \to \bar{d}$ in $C^1[0,1]$ as $j \to \infty$. Clearly, $\bar{d}(x) \geqslant c_1$ for all $x \in [0,1]$ and $t_0 \int_0^1 \frac{1}{d(z)} dz \leqslant q$, so that we can use the arguments of Theorem 1 to solve (2.8)–(2.11) for $t \geqslant t_0$ with initial data $\bar{d}$. □

Remark 3 We note that the condition $t \int_0^1 \frac{1}{d(x,t)} dt$ being less than 1 is equivalent to a bounded slope for u_x at $x = 1$. The condition $u_x(1,t) = \infty$ is associated with the flattening of the sheet against the vertical mould wall and hence with contact of the sheet on the wall $x = 1$. In order to continue with the physical solution we would need to impose a contact condition for the sheet at $x = 1$. We discretize a version of this in Section 4.2.

Remark 4 As the sheet stretches it thins globally and a simple condition on the initial thickness (satisfied by a uniform initial sheet) can be given which guarantees pointwise thinning for all time. If we assume that $d_0'(x) \geqslant 0$ for all $x \in [0,1]$ we obtain

$$d_t(x,t) \leqslant 0, \quad \forall\ (x,t) \in [0,1] \times [0,T].$$

Proof We use the same proof as for Theorem 1 replacing the set $\mathscr{B}$ by

$$\tilde{\mathscr{B}} := \{d \in \mathscr{B},\ d_t(x,t) \leqslant 0 \quad \forall\ (x,t) \in [0,1] \times [0,T]\}.$$

We only have to verify that $\mathscr{F}(\tilde{\mathscr{B}}) \subset \tilde{\mathscr{B}}$. Let $d \in \tilde{\mathscr{B}}$, since $d_t \leqslant 0$ the formulae (3.8) yield

$$u_x \geqslant 0, \quad u_t \leqslant 0, \quad u_{tx} \geqslant 0 \tag{3.31}$$

and therefore in view of (3.13) and (3.8)

$$b(x,t) \geqslant 0, \quad g(x,t) \leqslant 0, \quad g_x(x,t) \geqslant 0. \tag{3.32}$$

Since $\frac{\partial\lambda}{\partial x} > 0$ using (3.19) we conclude $e_x(x,t) \geqslant 0$ for all $(x,t) \in [0,1] \times [0,T]$ and hence

$$e_t(x,t) = g(x,t) - b(x,t)e_x(x,t) \leqslant 0,$$

so that again $e = \mathscr{F}(d) \in \tilde{\mathscr{B}}$. □

Remark 5 We define below a $T_{\max}$ which we expect to be the time at which the solution fails to exist and derive lower and upper bounds for it. Let $d_0(x) = 1$ for $x \in [0,1]$ and define

$$T_{\max} := \sup\Big\{ t \,|\, \inf_{x\in[0,1]} d(x,t) > 0, t\int_0^1 \frac{1}{d(z,t)}dz < 1\Big\}.$$

Then $T_{\max} \in (\frac{1}{\sqrt{3}}, 1)$.

Proof Let us first show that $T_{\max} > \frac{1}{\sqrt{3}}$. To this end define

$$\bar t := \sup\Big\{ t > 0 \,|\, d,u \in C^1([0,1]\times[0,t]) \text{ solve } (2.8)-(2.11) \text{ and } \inf_{x\in[0,1]} d(x,t) > \frac{2}{3}\Big\}.$$

Clearly, $\bar t > 0$, and assume that $\bar t < \frac{1}{\sqrt{3}}$. Since $\bar t \int_0^1 \frac{1}{d(z,t)}dz \leqslant \frac{1}{\sqrt{3}}\frac{3}{2} < 1$ for all $t < \bar t$, Remark 2 implies that the solution (d,u) exists beyond $\bar t$, so that we must have $\inf_{x\in[0,1]} d(x,\bar t) = \frac{2}{3}$. Using (3.14) and (3.13) and observing that $d_0(x) = 1, x \in [0,1]$ we may write for $t < \bar t$

$$d(x,t) = 1 + \int_0^t g(\lambda(s;x,t),s)ds = 1 + \int_0^1 s\frac{u_t(\lambda(s;x,t),s)}{\sqrt{1+u_x^2(\lambda(s;x,t),s)}}ds.$$

Since $u_t \leqslant 0, u_{tx} \geqslant 0$ by Remark 4, we further conclude

$$\begin{aligned} d(x,t) &\geqslant 1 + \int_0^t s u_t(\lambda(s;x,t),s)ds \geqslant 1 + t\int_0^t u_t(\lambda(s;x,t),s)ds \\ &\geqslant 1 + t\int_0^t u_t(0,s)ds = 1 + tu(0,t) = 1 - t\int_0^1 \frac{t\alpha(z,t)}{\sqrt{1-t^2\alpha^2(z,t)}}dz \end{aligned}$$

by (3.6) and since $u(x,0) = 0, x \in [0,1]$. Since $\inf_{x\in[0,1]} d(x,t) > \frac{2}{3}$ for $t < \bar t$ we obtain

$$\alpha(z,t) = \int_0^z \frac{1}{d(s,t)}ds < \frac{3}{2}z, \qquad t < \bar t,$$

and therefore

$$d(x,t) > 1 - t\int_0^1 \frac{\frac{3}{2}tz}{\sqrt{1-t^2(\frac{3}{2}z)^2}}dz = 1 - \frac{2}{3}\Big(1 - \sqrt{1-t^2(\frac{3}{2})^2}\Big) = \frac{1}{3} + \frac{2}{3}\sqrt{1-t^2(\frac{3}{2})^2}.$$

If we let $t \nearrow \bar t$ and recall that $\inf_{x\in[0,1]} d(x,\bar t) = \frac{2}{3}$ we obtain

$$\frac{2}{3} \geqslant \frac{1}{3} + \frac{2}{3}\sqrt{1-\bar t^2(\frac{3}{2})^2} > \frac{1}{3} + \frac{2}{3}\sqrt{1-\frac{1}{3}(\frac{3}{2})^2} = \frac{2}{3},$$

which is a contradiction. This proves that $\bar t \geqslant \frac{1}{\sqrt{3}}$ and using Remark 2 again, the solution (d,u) can be extended to some interval $[0, \frac{1}{\sqrt{3}} + \delta)$. As a result $T_{\max} > \frac{1}{\sqrt{3}}$.
Finally, observing that $d_0(x) = 1, x \in [0,1]$ and that $d_t \leqslant 0$ by Remark 4, we infer $t\int_0^1 \frac{1}{d(z,t)}dz \geqslant t$ so that $T_{\max} \leqslant 1$. □

4 Numerical discretization of the graph formulation

In this section we present discretizations of the models derived in Section 1 and 2.

4.1 The one-dimensional mould-free graph formulation

We begin with a discretization of the one-dimensional mould-free model (2.8)–(2.11). Let $x_j = jh$, $j = 0, \ldots, J$ be a uniform grid with mesh size $h = 1/J$ and $t_n = n\Delta t$, where $\Delta t > 0$ is the time step. We denote by (d_j^n, u_j^n) the approximations to $(d(x_j, t_n), u(x_j, t_n))$. Suppose (d_j^n, u_j^n) is given, then u_j^{n+1}, $j = 0, \ldots, J$ is found with the help of standard semi-implicit finite differences

$$\frac{u_{j+1}^{n+1} - u_j^{n+1}}{hq_{j+1}^{n+1}} - \frac{u_j^{n+1} - u_{j-1}^{n+1}}{hq_j^{n+1}} = \frac{hP(t_{n+1})}{d_j^n} \qquad \forall\ j \in [0, J-1] \tag{4.1}$$

$$u_{-1}^{n+1} = u_1^{n+1},\ u_J^{n+1} = 0 \tag{4.2}$$

where

$$q_j^n = \sqrt{1 + \left(\frac{u_j^n - u_{j-1}^n}{h}\right)^2} \qquad \forall\ j \in [0, J].$$

We solve (4.1)–(4.2) at each time step by an iterative procedure; we take an initial guess for q_j^n and then we use successive over relaxation to solve (4.1) as a linear system with q_j^n evaluated using the values of u_j^n from the previous iteration. We then use a standard upwinding explicit finite difference scheme to approximate (2.10) resulting in the following,

$$\frac{d_j^{n+1} - d_j^n}{\Delta t} + [v_j^n]_+ \frac{d_j^n - d_{j-1}^n}{h} + [v_j^n]_- \frac{d_{j+1}^n - d_j^n}{h} = f_j^n \quad j \in\ [0, J] \tag{4.3}$$

where $[a]_+ = \max(a, 0)$, $[a]_- = \min(a, 0)$

$$v_j^n = -\frac{(u_{j+1}^n - u_{j-1}^n)(u_j^{n+1} - u_j^n)}{2h\,(\hat{q}_j^n)^2\,\Delta t}, \quad f_j^n = \frac{(u_j^{n+1} - u_j^n)P(t_n)}{\hat{q}_j^n\,\Delta t},$$

while

$$\hat{q}_j^n = \sqrt{1 + \left(\frac{u_{j+1}^n - u_{j-1}^n}{2h}\right)^2} \qquad \forall\ j \in [0, J-1].$$

Note that $v_0^n = v_J^n = 0, f_J^n = 0$ by (4.2). For the initial data (2.11) we set

$$u_j^0 = 0, \quad d_j^0 = d_0(x_j), \quad \forall\ j \in\ [0, J]. \tag{4.4}$$

For stability of the scheme (4.3) we impose the usual stability condition for a first order equation,

$$\frac{\Delta t}{h} \max_{j \in [0,J]} |v_j^n| \leqslant 1. \tag{4.5}$$

If the spatial differences in (4.3) are evaluated at the level $n+1$ then the scheme would be unconditionally stable. The resulting linear equations would be easily solvable using the specific tridiagonal structure. In all the computations shown in § 6 we ensure that (4.5) is satisfied.

4.2 The one-dimensional graph formulation of the contact problem

In this section we numerically solve (2.19) in one space dimension for $P(t) = t$, $d_0(x) = 1, x \in [0, 1]$ and an obstacle ψ which is given as a negative constant. Clearly, the solution of this problem will initially coincide with the solution to the mould-free problem. Numerical

calculations show that if we choose $\psi = -1$, then the sheet hits the obstacle at some time t_1 before the slope at the right endpoint becomes infinite (which occurs say at time $t_2 > t_1$). At time $t = t_2$ the solution looses the property of being a graph and in order to follow the evolution for $t \geqslant t_1$ in a graph setting we rotate our coordinate system as indicated in Figure 3, writing

$$(\xi, \eta) = \frac{1}{\sqrt{2}}(x + y + 1, -x + y + 1).$$

Note that in Figure 3 the dotted lines denote the horizontal and vertical walls of a rectangular mould.

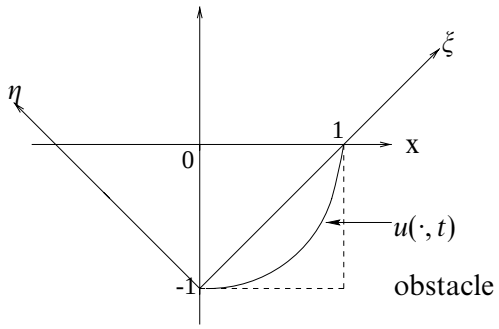

FIGURE 3. Change of variables

Since $x \mapsto u(x, t_1)$ is strictly increasing and $-1 \leqslant u(x, t_1) \leqslant 0$ for all $x \in [0, 1]$, for every $\xi \in [0, \sqrt{2}]$ there exists a unique $x = x(\xi) \in [0, 1]$ with $\xi = \frac{1}{\sqrt{2}}(x + u(x, t_1) + 1)$. Letting $\tilde{d}_1(\xi) := d(x(\xi), t_1)$, $\xi \in \tilde{\Omega} = [0, \sqrt{2}]$ we set up the following transformed problem for $t \geqslant t_1$:

$$\int_{\tilde{\Omega}} \frac{\tilde{u}_\xi}{\sqrt{1 + \tilde{u}_\xi^2}}(\tilde{\eta}_\xi - \tilde{u}_\xi) + \int_{\tilde{\Omega}} \frac{t}{\tilde{d}}(\tilde{\eta} - \tilde{u}) \geqslant 0 \qquad \forall\, \tilde{\eta} \in \tilde{K}, t > t_1 \tag{4.6}$$

$$\tilde{u}_\xi(0, t) = -1, \quad \tilde{u}(\sqrt{2}, t) = 0 \qquad \forall\, t > t_1 \tag{4.7}$$

$$\tilde{d}_t + \tilde{v}\tilde{d}_\xi = \frac{t\tilde{u}_t}{\sqrt{1 + \tilde{u}_\xi^2}} \quad \forall\, \xi \in \tilde{\Omega}, t > t_1 \tag{4.8}$$

$$\tilde{d}(\xi, t_1) = \tilde{d}_1(\xi) \qquad \forall\, \xi \in \tilde{\Omega} \tag{4.9}$$

where

$$\tilde{K} = \{\tilde{\eta} \in H^1(\tilde{\Omega}) \,|\, \tilde{\eta}(\xi) \geqslant \tilde{\psi}(\xi) \quad \forall\, \xi \in \tilde{\Omega}, \quad \tilde{\eta}(\sqrt{2}) = 0\}$$

and

$$\tilde{v} = -\frac{\tilde{u}_\xi \tilde{u}_t}{1 + \tilde{u}_\xi^2}, \qquad \tilde{\psi}(\xi) = \begin{cases} -\xi & 0 \leqslant \xi \leqslant \frac{\sqrt{2}}{2} \\ \xi - \sqrt{2} & \frac{\sqrt{2}}{2} < \xi \leqslant \sqrt{2}. \end{cases}$$

Next we describe our numerical method starting with the discretization of (2.19) in one space dimension. We use the same notation as in § 4.1 as well as

$$u_h^n(x) = \sum_{j=0}^{J} u_j^n \chi_j(x), \quad d_h^n(x) = \sum_{j=0}^{J} d_j^n \chi_j(x),$$

where $\chi_j(x)$ is the standard piecewise linear basis function. A numerical scheme for (2.19) in one space dimension takes the form: given (d_h^n, u_h^n), solve first

$$\int_\Omega \frac{u_{hx}^{n+1}(\eta_x - u_{hx}^{n+1})}{\sqrt{1+(u_{hx}^{n+1})^2}}\, dx + \int_\Omega I_h\Big(\frac{t_{n+1}}{d_h^n}(\eta - u_h^{n+1})\Big) dx \geqslant 0 \ \forall \eta \in K_h \tag{4.10}$$

$$u_{-1}^{n+1} = u_1^{n+1}, u_J^{n+1} = 0, \tag{4.11}$$

where I_h is the usual Lagrange interpolation operator and

$$K_h = \{\eta \in S_h : \eta(x_j) \geqslant \psi(x_j), \quad \forall\ j = 0, \ldots, J-1,\ \eta_J = 0\}.$$

It is well known that the solution of the discrete obstacle problem (4.10), (4.11) can be obtained in the following way; first we calculate an explicit update $\bar{u}_h^{n+1}$ by solving (4.4) with u_j^{n+1} replaced by $\bar{u}_j^{n+1}$. Then, $u_h^{n+1} = \sum_{j=0}^{J} u_j^{n+1}\chi_j$ with

$$u_j^{n+1} = \max\,(\bar{u}_j^{n+1}, \psi_j), \quad j \in [0, J] \tag{4.12}$$

is a solution of (4.10), (4.11). Afterwards we use (4.3) in order to calculate d_h^{n+1} from u_h^n, u_h^{n+1}. This is done until we reach a point $\tilde{T} = \tilde{N}\Delta t$ at which the sheet hits the obstacle for the first time. This happens at the left endpoint of our interval, so that $u_0^{\tilde{N}} = -1$. Now we proceed just as described at the beginning of this section, transforming our problem to new coordinates, in which the solution remains a graph. In the discrete setting we define

$$\xi_j = \frac{1}{\sqrt{2}}(x_j + u_j^{\tilde{N}} + 1), \qquad j = 0, \ldots, J.$$

Clearly, $\xi_0 = 0, \xi_J = \sqrt{2}$ but in general these gridpoints will not be equally spaced. We therefore introduce the points $\tilde{\xi}_j = j\tilde{h}$, $j = 0, \ldots, J, \tilde{h} = \frac{\sqrt{2}}{J}$ and set for $j \in [0, J]$

$$(\tilde{d}_j^{\tilde{N}}, \tilde{u}_j^{\tilde{N}}) := \alpha(d_k^{\tilde{N}}, u_k^{\tilde{N}}) + (1-\alpha)(d_{k+1}^{\tilde{N}}, u_{k+1}^{\tilde{N}}) \quad \text{if } \tilde{\xi}_j = \alpha\xi_k + (1-\alpha)\xi_{k+1}, \alpha \in [0,1].$$

The calculation is continued in the same way as above, the only difference being that the discretization of (2.19) in one space dimension is replaced by the corresponding discretization of (4.6)–(4.9).

5 The parameterised contact problem

5.1 Formulation

In what follows we assume that $\partial\mathscr{M} \in C^2$. It is well-known that there exists $\rho > 0$ such that the signed distance function

$$d_{\mathscr{M}}(\mathbf{x}) := \begin{cases} -\mathrm{dist}(\mathbf{x}, \partial\mathscr{M}), & \mathbf{x} \in \mathscr{M} \\ \mathrm{dist}(\mathbf{x}, \partial\mathscr{M}), & \mathbf{x} \notin \mathscr{M} \end{cases}$$

is in $C^2(N_\rho)$, where $N_\rho := \{\mathbf{x} \in \mathbb{R}^2 \mid \operatorname{dist}(\mathbf{x}, \partial\mathscr{M}) < \rho\}$. Furthermore, for every $\mathbf{x} \in N_\rho \setminus \mathscr{M}$ there exists a unique $\mathbf{y} \in \partial\mathscr{M}$ such that

$$\mathbf{x} = \mathbf{y} + d_{\mathscr{M}}(\mathbf{x})\boldsymbol{\nu}_{\mathscr{M}}(\mathbf{y}), \tag{5.1}$$

and $\nabla d_{\mathscr{M}}(\mathbf{x}) = \boldsymbol{\nu}_{\mathscr{M}}(\mathbf{y})$. Using this last relation we may write (1.4), (1.5) in complementarity form as

$$d_{\mathscr{M}}(\mathbf{x})\mathbf{R} = 0,\ d_{\mathscr{M}}(\mathbf{x}) \leqslant 0,\quad \mathbf{R} \cdot \nabla d_{\mathscr{M}}(\mathbf{x}) \geqslant 0, \mathbf{x} \in \Gamma. \tag{5.2}$$

A fixed point formulation of the system is obtained by introducing the projection $P_{\mathscr{M}} : N(\mathscr{M}) = \mathscr{M} \cup N_\rho \to \mathbb{R}$ by

$$P_{\mathscr{M}}(\mathbf{x}) := \begin{cases} \mathbf{x}, & \mathbf{x} \in \overline{\mathscr{M}} \\ \mathbf{y}, & \mathbf{x} \in N(\mathscr{M})\setminus\overline{\mathscr{M}},\ \mathbf{y} \text{ as in (5.1).} \end{cases}$$

It follows that if for any $\mu > 0$ and $\mathbf{R}$ such that $\mathbf{x} + \mu\mathbf{R} \in N(\mathscr{M})$ a solution of the fixed point problem

$$\mathbf{x} = P_{\mathscr{M}}(\mathbf{x} + \mu\mathbf{R}) \tag{5.3}$$

satisfies the complementarity system (5.2). This holds because $P_{\mathscr{M}}(N(\mathscr{M})) = \overline{\mathscr{M}}$ and since

$$\begin{aligned} \mathbf{x} \in \mathscr{M} \quad &\Rightarrow \quad \mathbf{x} = \mathbf{x} + \mu\mathbf{R} \quad &&\Rightarrow \quad \mathbf{R} = 0, \\ \mathbf{x} \in \partial\mathscr{M} \quad &\Rightarrow \quad \mathbf{x} + \mu\mathbf{R} \in N(\mathscr{M}) \setminus \mathscr{M} \quad &&\Rightarrow \quad \mu\mathbf{R} \cdot \boldsymbol{\nu}_{\mathscr{M}}(\mathbf{x}) \geqslant 0, \end{aligned}$$

which implies (5.2).

Writing the curve Γ as $\mathbf{x}(p,t)$, $p \in [0,1]$ we observe that

$$\mathbf{R} = \frac{1}{|\mathbf{x}_p|}\frac{\partial}{\partial p}\left(\frac{\mathbf{x}_p}{|\mathbf{x}_p|}\right) - \frac{P(t)}{d(p,t)}\frac{\mathbf{x}_p^\perp}{|\mathbf{x}_p|}, \qquad p \in (0,1) \tag{5.4}$$

where $\mathbf{a}^\perp = (-a_2, a_1)$ for $\mathbf{a} = (a_1, a_2) \in \mathbb{R}^2$. The equation for mass conservation is given by (1.8) while the condition that the sheet evolves in the normal direction is given by (1.9). In the case of contact with the mould when the material reaches the mould wall further movement is prevented and to model this we use the same approach as in Chapman *et al.* [3] and assume that the material sticks to the mould on contact and does not move thereafter.

From (1.8) we infer

$$\frac{d_t}{d} = -\frac{1}{|\mathbf{x}_p|^2}\mathbf{x}_p \cdot \mathbf{x}_{pt}$$

and differentiating (1.9) with respect to p implies

$$\mathbf{x}_p \cdot \mathbf{x}_{pt} = -\mathbf{x}_t \cdot \mathbf{x}_{pp}.$$

We combine these equations to yield

$$\frac{d_t}{d} = \frac{1}{|\mathbf{x}_p|^2}\mathbf{x}_t \cdot \mathbf{x}_{pp}, \tag{5.5}$$

which gives the evolution equation for the thickness of the sheet. The problem is then to

find $\{\mathbf{x}, d\}$ such that (5.3), (5.4), (5.5) hold together with the boundary conditions

$$\mathbf{x}(0,t) = (-1,0), \quad \mathbf{x}(1,t) = (1,0), \quad t \in [0,T] \tag{5.6}$$

and the initial conditions

$$\mathbf{x}(p,0) = x_0(p) = (-1+2p,0), \quad d(p,0) = d_0(p), \quad p \in [0,1]. \tag{5.7}$$

5.2 Discretization

Consider a discrete approximation $\{\mathbf{x}_j^n, d_j^n\}_{j=0}^{j=J}$ to $\{\mathbf{x}(p,t^n), d(p,t^n)\}$ where $t^n = n\Delta t$. The initial and boundary conditions (5.7) and (5.6) are approximated by

$$\mathbf{x}_j^0 = \left(-1+\frac{2j}{J},0\right), \quad d_j^0 = d_0\left(\frac{j}{J}\right), \quad j \in [0,J] \tag{5.8}$$

$$\mathbf{x}_0^n = (-1,0), \quad \mathbf{x}_J^n = (1,0). \tag{5.9}$$

We set

$$h_j^n = \frac{1}{2}|\mathbf{x}_{j+1}^n - \mathbf{x}_{j-1}^n|, \; h_{j+1/2}^n = |\mathbf{x}_{j+1}^n - \mathbf{x}_j^n|$$

and

$$\begin{aligned}\mathbf{R}_j^n &= \frac{1}{h_j^{n-1}}\left(\frac{\mathbf{x}_{j+1}^n - \mathbf{x}_j^n}{h_{j+1/2}^{n-1}} - \frac{\mathbf{x}_j^n - \mathbf{x}_{j-1}^n}{h_{j-1/2}^{n-1}}\right) - \frac{P^n}{d_j^{n-1}}\left(\frac{(\mathbf{x}_{j+1}^n)^\perp - (\mathbf{x}_{j-1}^n)^\perp}{2h_j^{n-1}}\right)\\ &=: \alpha_j^n \mathbf{x}_j^n + \beta_j^n \mathbf{x}_{j-1}^n + \gamma_j^n \mathbf{x}_{j+1}^n + \delta_j^n (\mathbf{x}_{j-1}^n)^\perp + \epsilon_j^n (\mathbf{x}_{j+1}^n)^\perp.\end{aligned}$$

We wish to find a solution of :-

$$\mathbf{x}_j^n = P_{\mathscr{M}}(\mathbf{x}_j^n + \mu \mathbf{R}_j^n) \tag{5.10}$$

and then update d_j^{n-1} by the discretization of (5.5)

$$\frac{d_j^n - d_j^{n-1}}{\Delta t} = d_j^{n-1}\frac{(\mathbf{x}_j^n - \mathbf{x}_j^{n-1})}{\Delta t} \cdot \frac{(\mathbf{x}_{j+1}^n - 2\mathbf{x}_j^n + \mathbf{x}_{j-1}^n)}{h_j^2}. \tag{5.11}$$

In order to solve (5.10) we use the projected Gauss–Seidel iteration

$$\begin{aligned}\tilde{\mathbf{x}}_j^{k+1} &= \mathbf{x}_j^k - \tfrac{1}{\alpha_j^n}\left(\alpha_j^n \mathbf{x}_j^k + \beta_j^n \mathbf{x}_{j-1}^{k+1} + \gamma_j^n \mathbf{x}_{j+1}^k + \delta_j^n (\mathbf{x}_{j-1}^{k+1})^\perp + \epsilon_j^n (\mathbf{x}_{j+1}^k)^\perp\right)\\ \mathbf{x}_j^{k+1} &= P_{\mathscr{M}}(\tilde{\mathbf{x}}_j^{k+1}),\end{aligned} \tag{5.12}$$

where we suppress the time step index and $\mathbf{x}_j^k$ represents the kth iterate. If this iteration converges then the limit $\mathbf{x}_j^n$ satisfies the complementarity problem

$$\mathbf{x}_j^n = P_{\mathscr{M}}(\mathbf{x}_j^n - \frac{1}{\alpha_j^n}\mathbf{R}_j^n)$$

which also yields a solution of (5.10), since $\alpha_j^n < 0$. In order to solve (5.12) we formulate a fixed point iteration for the nonlinear equations which define $P_{\mathscr{M}}(\hat{\mathbf{x}}_j^{k+1})$ in the case of the lower part of the mould being the graph $\{y = \psi(x)\}$. Furthermore in the calculations we use the hypothesis that once the sheet hits the mould wall it remains attached to the mould so if $\mathbf{x}_j^n \in \partial\mathscr{M}$ we fix its position on the mould for all subsequent time steps.

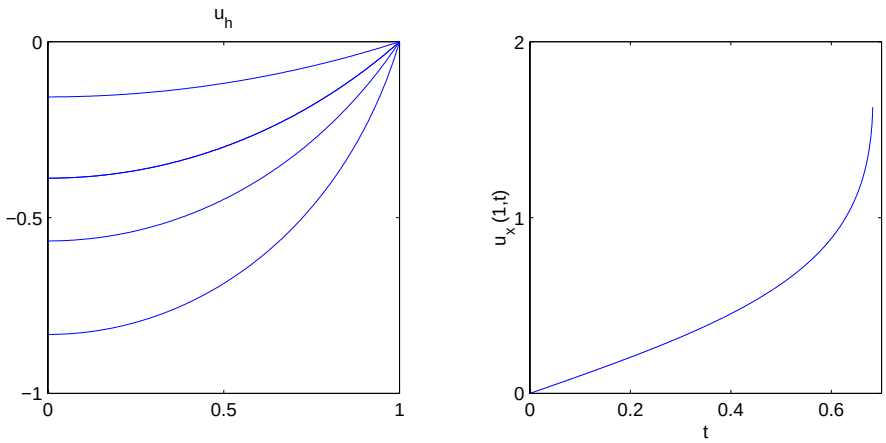

FIGURE 4. The sheet u_h together with $(u_h(1,t))_x$ plotted against t.

We note that this is a semi-implicit scheme. Since locally in space (5.5) is an ordinary differential equation for d, we use a standard condition for the explicit Euler method

$$\Delta t \leqslant \frac{|\mathbf{x}_j^n - \mathbf{x}_j^{n-1}|}{\Delta t} \frac{|\mathbf{x}_{j+1}^n - 2\mathbf{x}_j^n + \mathbf{x}_{j-1}^n|}{h_j^2},$$

to ensure d_j^n decreases in time. Note that this essentially says that Δt is sufficiently small independent of the spatial mesh but dependent on the solution of the problem. It is just as convenient to replace d_j^{n-1} in the right hand side of (5.11) with d_j^n. The numerical discretization in Chapman et al. [3] involves a finite difference approximation of (1.7) and (1.9). Moreover d is eliminated by integrating (1.8) with respect to time. The discrete version of (1.7) and (1.9) becomes the equation for the components of $\mathbf{x}_j^n$. The scheme is again semi-implicit and the authors report that stability of the scheme is not an issue.

6 Numerical results

In this section we display numerical approximations of solutions to the models presented in Sections 1 and 2. Without loss of any information we take $P(t) = t$. In all one-dimensional simulations we use the discretizations derived in § 4 with, unless otherwise stated, $J = 201 \Rightarrow h = 1/200$ and $\Delta t = 1/800$ for the graph discretizations and $J = 201$ and $\Delta t = (1/100)^2/40$ for the parametric discretizations. Furthermore we always take the initial thickness to be a uniform constant for which we take a scaling such that $d_0 = 1$ without loss of generality. The choice of time step is guided by accuracy rather than stability considerations. This is because the evolutionary equation is either a first order partial differential equation or an ordinary differential equation. In our computations the breakdown of the numerical solution was due to the loss of existence of solutions.

We display four sets of results. The first set, Figures 4–7, are simulations obtained using the one-dimensional discretizations of the graph formulation given in § 4.1 and 4.2.

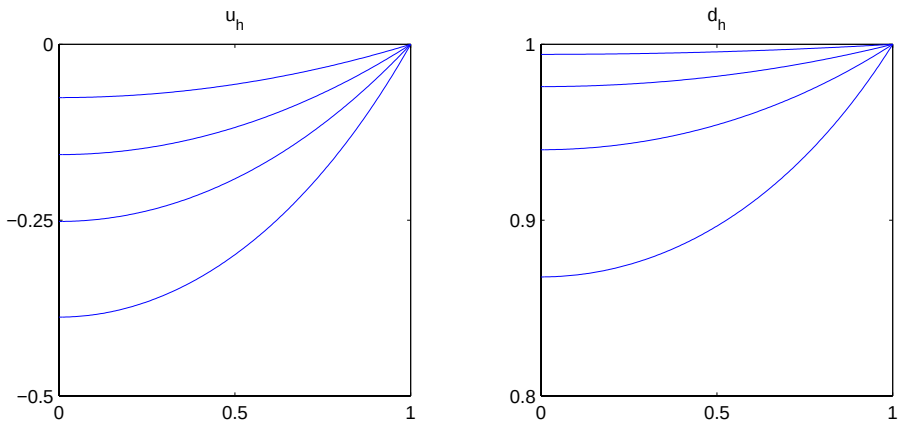

FIGURE 5. The sheet u_h and its thickness d_h evolving in time with no obstacle.

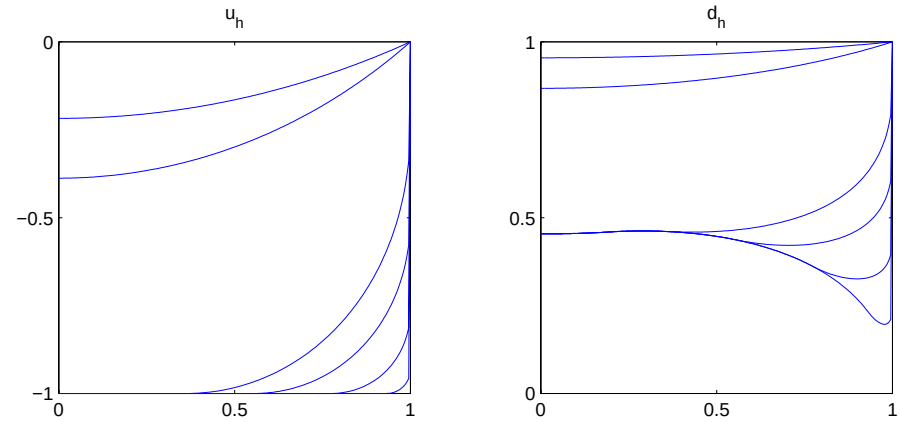

FIGURE 6. The sheet u_h and its thickness d_h evolving in time with obstacle $\psi(x) \equiv -1$.

The second set, Figures 8 and 9, are simulations obtained using the one-dimensional discretization of the parametric formulation given in § 5. We note that on the scales shown comparing the graph simulations in Figures 4–7 with the corresponding parametric simulations gives almost identical results and hence we do not include these parametric results. The third set, Figure 10 displays a backwards in time simulation of the one-dimensional mould-free set-up obtained by setting $\Delta t = -\Delta t$ in the discretization presented in § 4.1. The last set, Figures 12 and 13, are two-dimensional simulations of the graph formulation of the contact problem obtained using a discretization of (2.19) similar to that described in § 4.2 for one dimension.

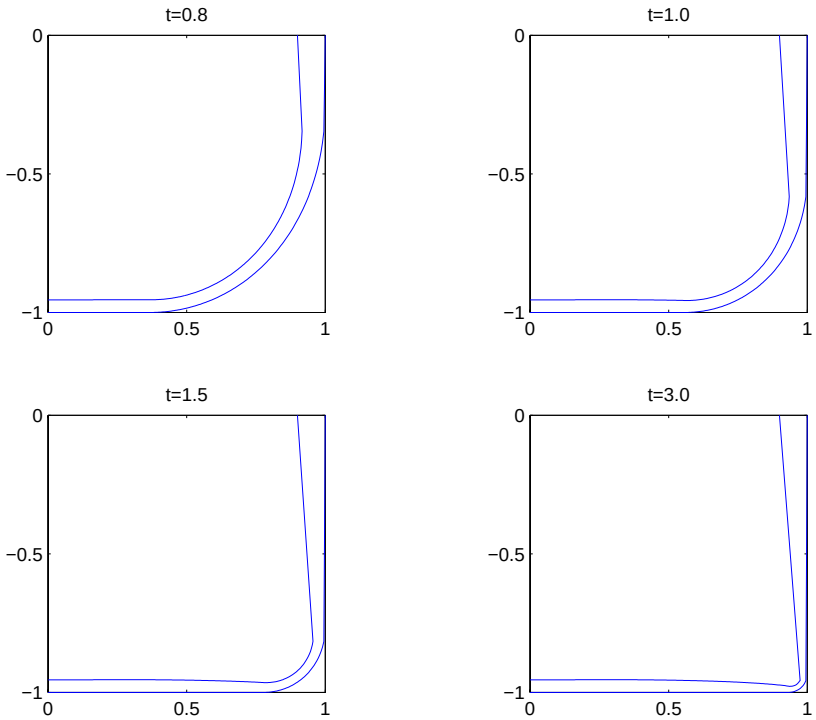

FIGURE 7. The sheet and its scaled thickness in the normal direction with obstacle $\psi(x) \equiv -1$.

6.1 One dimensional results

The left-hand plot in Figure 4, shows the evolution of the sheet u_h in the mould-free set-up with monotone increasing pressure. We see that as t increases from $t = 0$ to $t = 0.68$ (the top three curves) the sheet begins to sink in the middle at a uniform rate, however as t increases during the short interval from 0.68 to 0.6829 (the third and fourth curves) the speed at which the sheet sinks in the middle increases dramatically. The right-hand plot in Figure 4 shows the gradient of the approximate solution u_h at the boundary $x = 1$, plotted against t, calculated using numerical integration of the formula for u_x in (3.8). We see that the slope of the graph remains finite for $0 \leqslant t \leqslant 0.65$, but as t approaches 0.68 it soon becomes infinite. In the computations displayed in Figure 4 we set $h = 1/200$ and $\Delta t = h^2/40$. We note that the value 0.68 is in accord with the bound on $T_{\max}$ in Remark 5 in § 3.

In Figure 5 we see the evolution of the sheet u_h and its thickness d_h in a mould-free configuration. We plot the solutions at the four values $t = 0.15, 0.3, 0.45$ and 0.6.

In Figure 6 we see the evolution of a sheet u_h and its thickness d_h plotted at times $t = 0.4$, 0.6, 0.8, 1.0, 1.5 and 3.0 in a configuration with a mould defined by $\psi \equiv -1$. These solutions are obtained from solving the discretization of the contact problem (2.19) in one space dimension until the approximate solution $u_h^n(0)$ hits the mould $\psi = -1$ at which point we solve the discretization of the change of variables problem (4.6)–(4.9)

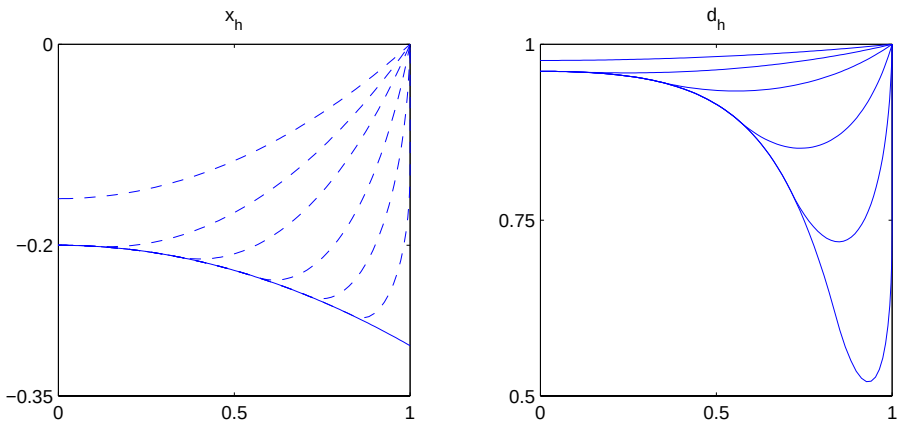

FIGURE 8. The sheet $\mathbf{x}_h$ and its thickness d_h evolving in time with obstacle $\psi(x) = 0.2 - 0.1x^2$.

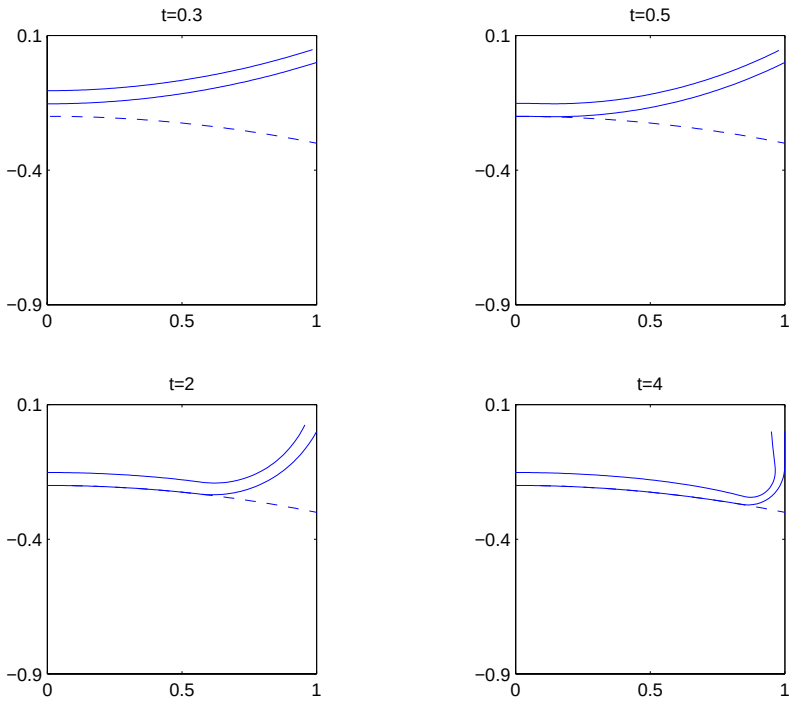

FIGURE 9. The sheet and its scaled thickness in the normal direction with obstacle $\psi(x) \equiv 0.2 - 0.1x^2$.

with $\tilde{\Omega} = [0, \sqrt{2}]$. Where necessary the approximate solutions have been changed back to the initial configuration. In Figure 7 we plot the sheet u_h against x (bold line) together with its scaled thickness in the normal direction. This gives a clearer idea of the actual thickness of the sheet in the mould.

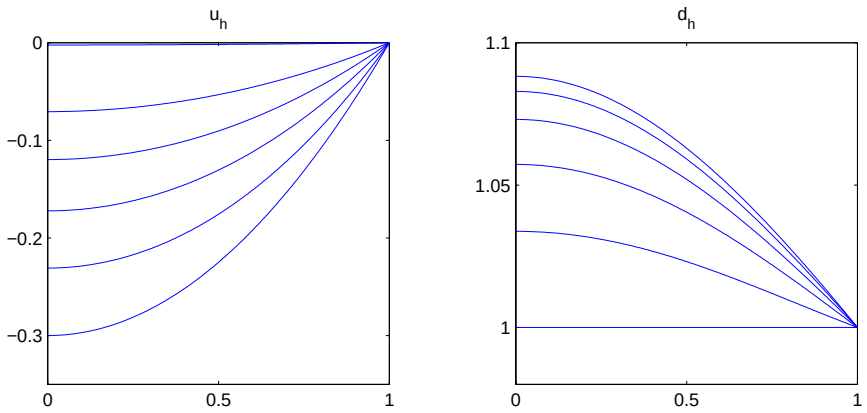

FIGURE 10. The sheet and its scaled thickness evolving backwards in time.

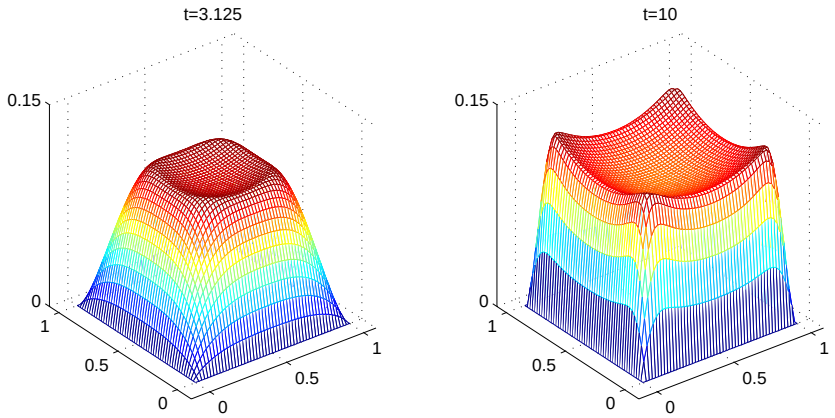

FIGURE 11. The sheet $-u_h$, evolving in time with obstacle $\psi(x, y) = -5.1 + \sqrt{25 - (x - 0.5)^2 - (y - 0.5)^2}$.

In Figures 8 and 9 we see the evolution of the sheet and its thickness for the contact problem with obstacle $\psi(x) = -0.2 - 0.1x^2$, obtained using the discretization of the parametric approach. The left-hand plot in Figure 8 displays the sheet (dashed line) together with the obstacle (bold line) at times $t = 0.3$, 0.5, 1, 2, 3, 4 and 6 while the right-hand plot displays its thickness. In Figure 9 we plot the sheet (bold line) together with its scaled thickness in the normal direction and the obstacle (dashed line) at times $t = 0.3$, 0.5, 2 and 4. Note that in Figures 8 and 9 although we solve the discretization on the interval $[-1, 1]$, due to the symmetry of the problem and in keeping with the graph simulations, we only display the approximate solutions on the interval $[0, 1]$.

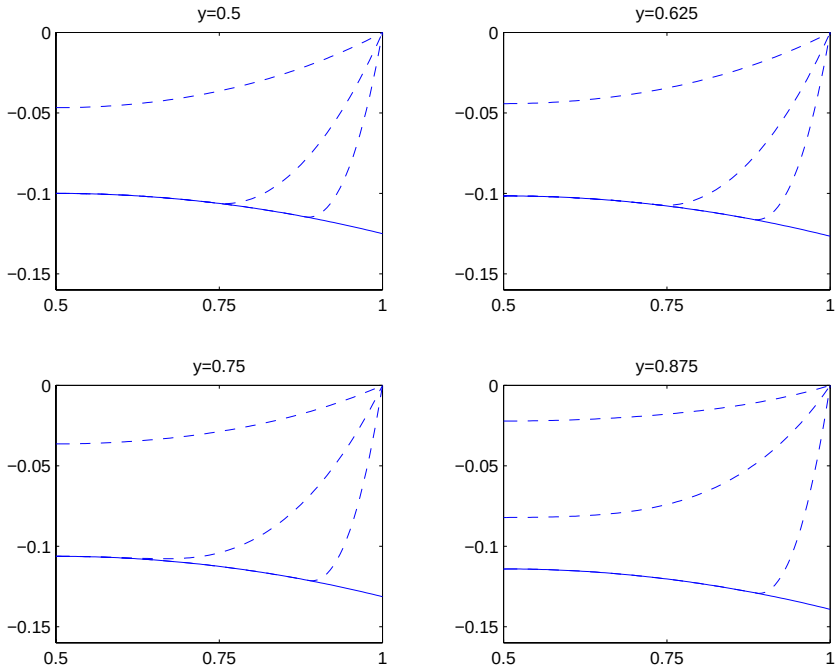

FIGURE 12. Cross-sectional plots of the sheet u_h, evolving in time with obstacle $\psi(x, y) = -5.1 + \sqrt{25 - (x - 0.5)^2 - (y - 0.5)^2}$.

For illustrative purposes, we conclude the one-dimensional computations with Figure 10 which displays a backward in time simulation of the sheet (lefthand subplot) and its thickness (righthand subplot) in the mould-free set-up. We take the final sheet to be an arc of a circle with uniform thickness by setting $P(t) = t$, the final time to be 0.45 and the final thickness to be 1. The solutions are plotted at times $t = 0.45$, 0.35, 0.25, 0.15 and 0.05. Note that since the applied pressure is zero at $t = 0$ the sheet is flat at this time whereas the thickness is non-uniform.

6.2 Two dimensional results

We conclude with some two-dimensional results for the contact problem (2.19) with $\Omega = (0, 1) \times (0, 1)$. The symmetry of the set-up enables us to solve our discretization on one quarter of the domain. The results displayed were solved on a uniform grid with $h = 1/200$, $\Delta t = h^2/40$ and $\psi = -5.1 + \sqrt{25 - (x - 0.5)^2 - (y - 0.5)^2}$. Figure 11 displays the sheet at times $t = 3.125$ and $t = 10$, in this figure instead of plotting the sheet u_h we plot $-u_h$ for the simple reason that this gives a better view of the sheet's contact with the mould.

For the two-dimensional results we display four cross-sectional plots, at $y = 0.5$, $y = 0.625$, $y = 0.75$ and $y = 0.875$, of the evolution of the sheet and its thickness. In Figure 12 we display the obstacle (a bold line) together with the sheet $u_h(x, t)$ at times

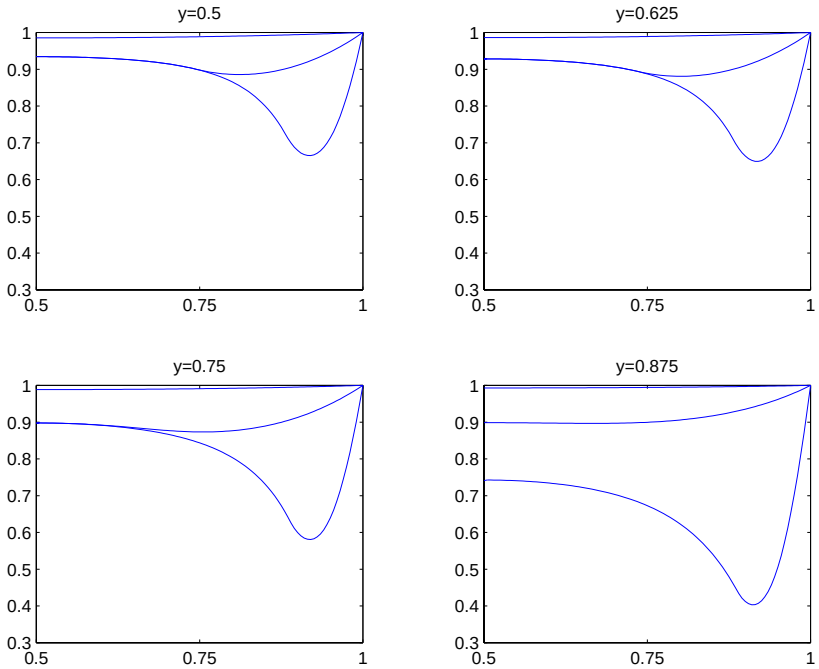

FIGURE 13. Cross-sectional plots of the sheet's thickness d_h, evolving in time with obstacle $\psi(x, y) = -5.1 + \sqrt{25 - (x - 0.5)^2 - (y - 0.5)^2}$.

$t = 0.625$, $t = 3.125$ and $t = 10$ (dashed lines) while Figure 13 displays the sheets thickness $d_h(x, t)$ at the aforementioned times. In these calculations the sheet does not make contact with the vertical mould wall.

7 Conclusion

We studied a mathematical model for the moulding of a superplastic sheet (due to Chapman *et al.* [3]) based on the assumptions that

(1) the deformation is quasi-static and the sheet is always in a critical plastic state leading to (1.1),

(2) the material in the sheet flows in a normal direction,

(3) upon contact with the rigid surface of the mould the sheet ceases to flow.

Using the local conservation of mass an evolution equation for the thickness of the sheet was derived. The mathematical problem was then formulated in both a parametric and a graph representation of the sheet as a coupled system of an elliptic equation for the surface and a first order evolution equation for the thickness of the sheet. This mathematical model is a significant simplification of the full system considered, for example, in [1, 2, 4], and should be more amenable to mathematical analysis and understanding. Indeed for

the graph formulation we were able to prove a local existence and uniqueness result as long as the sheet was not in contact with the mould. The proof was based on a fixed point argument using the contraction mapping principle.

In our numerical computations we employ both the parametric and graph formulations. For the simple one-dimensional problems we considered in which the sheet remains a graph we discovered that the numerical methods gave essentially identical results for fine meshes. The graph formulation has the advantage of simplicity, the existence of a mathematical analysis and is computationally less expensive since it requires just one function to define the curve. On the other hand the parametric formulation allows the sheet to lose its graphlike property and hence is more generally applicable. However in the case of the contact problem one has to be careful in its implementation. It is not as straightforward as the discretization of the obstacle problem for a graph. The projection onto the admissable set of displacements leads to a nonconvex problem and hence a loss of global uniqueness. Also in the evolution process we found it convenient to fix the sheet once it was in contact with the mould.

From the mathematical point of view it would be interesting to:-

(1) develop the parametric formulation and its numerical discretization in three space dimensions,

(2) develop an existence theory for the parametric formulation and the contact problem,

(3) study the inverse problem in which one asks what is the initial shape and thickness of a sheet which yields a given final thickness and shape.

Furthermore since this mathematical model leads to a relatively simple computational problem with significantly fewer material parameters and constitutive relations it would be interesting from the point of view of industrial applications to compare the use of this model with experiments and other computational simulations.

Acknowledgement

Vanessa Styles was supported in this work by a Leverhulme Trust Special Research Fellowship.

References

[1] Bonet, J., Wood, R.D. & Wargadipura, A.H.S. (1990) *Numerical simulation of the superplastic forming of thin sheet components using the finite element method*, Int. J. Num. Meth. Eng. **30** 1719-1737.

[2] Carrino, L. & Guilliano, G. (1997) *Modelling of superplastic blow forming*, Int. J. Mech. Sci. **39** 193-199.

[3] Chapman, S. J., Fitt, A. D. & Pulos, G. C. (1999) *Vacuum moulding of a superplastic in two dimensions*, IMA J. Appl. Math. **63** 217-246.

[4] Doltsinis, I.S. (1995) *Numerical analysis and design of industrial superplastic forming* J. de Physique IV **37** 473-483.